VI International Conference on Particle-based Methods – Fundamentals and Applications
PARTICLES 2019
E. Oñate, M. Bischoff, D.R.J. Owen P. Wriggers, , & T. Zohdi (Eds)

GRANULAR FLOW ANALYSIS CONSIDERING SOIL STRENGTH USING MOVING PARTICLE SIMULATION METHOD

KAZUHIRO KANEDA[1] AND TOMOKI SAWADA[2]

[1] Takenaka R&D Institute
1-5-1 Ohtsuka, Inzai, Chiba 270-1395, Japan
E-mail: kaneda.kazuhiro@takenaka.co.jp website: https://www.takenaka.co.jp/takenaka_e/

[2] Prometech Software, Inc.
34-3, Hongo 3-chome, Bunkyo-ku, Tokyo 113-0033, Japan
E-mail sawada@prometech.co.jp, website: https://www.prometech.co.jp/

Key words: Granular flow analysis; MPM; Soil strength.

Abstract. In recent years, many sediment-related disasters have occurred in Japan. To predict the sediment flow, granular flow analysis was conducted with the moving particle simulation method, using the viscosity term formulated by the Drucker-Prager model. The program code used is Particleworks Ver. 6, developed by Prometech Software. Plastic viscosity is described as a function of (cohesion) c and Φ (the shear resistance angle). Simple problems, such as freestanding height and dam breakage of the simulations were analyzed to assess the accuracy of the particle simulation method with the model.

1 INTRODUCTION

Soil-related disasters occur frequently in Japan. After such occurrences, simulation analysis can be performed on the soil flow area to determine what factors lead to the disaster. The discrete element method (DEM), or particle method, can be employed by assuming soil to be the Bingham model. Dent et al. (1983) simulated an avalanche flow, involving snow and not soil, by assuming snow as the Bingham model. Subsequently, Soussa and Voight (1991) and Moriguchi et al. (2009) applied the particle method to soil flows. Nonoyama et al. (2015) also used simulation, with Smoothed Particle Hydrodynamics (SPH), for soil collapse analysis. Various other numerical analysis methods of collapsed systems are available, each with their own characteristics. In the current study, the collapse analysis was examined with the Moving Particle Simulation (MPS) particle method, originally developed by Koshizuka et al. (1996). This method is known to be able to solve stability for simulation, such as free surface flow. On the other hand, although soil can be assumed as a viscous fluid, such as in the Bingham model, the viscosity is considered inconstant as it can be changed by shear strain and soil constraint pressure. Focusing on this aspect, Moriguchi et al. (2009) proposed a "new" viscosity. Because viscosity changes with stress, it was necessary to modify the basic equation. In this study, therefore, the viscosity proposed by Moriguchi et al. (2009) is used. The basic equation is modified from the original and the behavior was investigated before and after modification.

2 FORMULATION OF THE MATHEMATICAL MODEL

The equivalent viscosity coefficient of the Bingham model proposed by Moriguchi et al. (2009) is as follows:

$$\eta' = \begin{cases} \eta_0 + \frac{c+p\tan\phi}{\sqrt{2V_{ij}V_{ij}}} (\eta \le \eta_{max}) \\ \eta_{max} \qquad (\eta > \eta_{max}) \end{cases} \tag{1}$$

where V_{ij} is the shear strain tensor.

$$V_{ij} = \frac{1}{2}\left(\frac{\partial u_i}{\partial x_j} + \frac{\partial u_j}{\partial x_i}\right) \tag{2}$$

where c is the cohesion (kPa), ϕ is the shear resistance angle ($^\circ$). The constitutive equation of fluid is as follows:

$$\sigma_{ij} = -p\delta_{ij} + 2\eta' V_{ij} = -p\delta_{ij} + \eta'\left(\frac{\partial u_i}{\partial x_j} + \frac{\partial u_j}{\partial x_i}\right) \tag{3}$$

where p is the pressure (kPa). The conservation of momentum is as follows:

$$\frac{\partial u_i}{\partial t} + u_j\frac{\partial u_i}{\partial x_j} = \frac{1}{\rho}\frac{\partial \sigma_{ij}}{\partial x_i} + g_i \tag{4}$$

where g (m/s) is the gravity acceleration. The uncompressed condition was considered.

$$\frac{\partial u_i}{\partial x_i} = 0 \tag{5}$$

Substitute Equation (4) for (3)

$$\frac{\partial u_i}{\partial t} + u_j\frac{\partial u_i}{\partial x_j} = -\frac{1}{\rho}\frac{\partial p}{\partial x_i} + \frac{1}{\rho}\frac{\partial}{\partial x_j}\left[\eta'\left(\frac{\partial u_i}{\partial x_j} + \frac{\partial u_j}{\partial x_i}\right)\right] + g_i \tag{6}$$

was obtained.
Ignoring the spatial gradient of the viscosity coefficient, it becomes a Navier-Stokes equation. However, in the current research, as a spatial gradient was needed, it was expanded by equation (6). Separate each term as follows:

$$\text{Advection term}: \frac{u_i^* - u_i^n}{\partial t} = -u_j\frac{\partial u_i}{\partial x_j} \tag{7}$$

$$\text{External force term}: \frac{u_i^{**} - u_i^*}{\partial t} = g_i \tag{8}$$

$$\text{Viscous term}: \frac{u_i^{***} - u_i^{**}}{\partial t} = \frac{1}{\rho}\frac{\partial}{\partial x_j}\left[\eta'\left(\frac{\partial u_i}{\partial x_j} + \frac{\partial u_j}{\partial x_i}\right)\right] \tag{9}$$

$$\text{Pressure term}: \frac{u_i^{n+1} - u_i^{***}}{\partial t} = -\frac{1}{\rho}\frac{\partial p}{\partial x_i} \tag{10}$$

Further expansion of the viscosity term is as follows:
X velocity:

$$\frac{1}{\rho}\left[\frac{\partial}{\partial x}\eta\left(\frac{\partial u_x}{\partial x}+\frac{\partial u_x}{\partial x}\right)+\frac{\partial}{\partial y}\eta\left(\frac{\partial u_x}{\partial y}+\frac{\partial u_y}{\partial x}\right)+\frac{\partial}{\partial z}\eta\left(\frac{\partial u_x}{\partial z}+\frac{\partial u_z}{\partial x}\right)\right] \tag{11}$$
$$=\frac{2}{\rho}\frac{\partial \eta}{\partial x}\frac{\partial u_x}{\partial x}+\frac{1}{\rho}\frac{\partial \eta}{\partial y}\left(\frac{\partial u_x}{\partial y}+\frac{\partial u_y}{\partial x}\right)+\frac{1}{\rho}\frac{\partial \eta}{\partial z}\left(\frac{\partial u_x}{\partial z}+\frac{\partial u_z}{\partial x}\right)$$

Y velocity:

$$\frac{1}{\rho}\left[\frac{\partial}{\partial x}\eta\left(\frac{\partial u_y}{\partial x}+\frac{\partial u_x}{\partial y}\right)+\frac{\partial}{\partial y}\eta\left(\frac{\partial u_y}{\partial y}+\frac{\partial u_y}{\partial y}\right)+\frac{\partial}{\partial z}\eta\left(\frac{\partial u_y}{\partial z}+\frac{\partial u_z}{\partial y}\right)\right] \tag{12}$$
$$=\frac{2}{\rho}\frac{\partial \eta}{\partial y}\frac{\partial u_y}{\partial y}+\frac{1}{\rho}\frac{\partial \eta}{\partial x}\left(\frac{\partial u_y}{\partial x}+\frac{\partial u_x}{\partial y}\right)+\frac{1}{\rho}\frac{\partial \eta}{\partial z}\left(\frac{\partial u_y}{\partial z}+\frac{\partial u_z}{\partial y}\right)$$

Z velocity:

$$\frac{1}{\rho}\left[\frac{\partial}{\partial x}\eta\left(\frac{\partial u_z}{\partial x}+\frac{\partial u_x}{\partial z}\right)+\frac{\partial}{\partial y}\eta\left(\frac{\partial u_z}{\partial y}+\frac{\partial u_y}{\partial z}\right)+\frac{\partial}{\partial z}\eta\left(\frac{\partial u_z}{\partial z}+\frac{\partial u_z}{\partial z}\right)\right] \tag{13}$$
$$=\frac{2}{\rho}\frac{\partial \eta}{\partial z}\frac{\partial u_z}{\partial z}+\frac{1}{\rho}\frac{\partial \eta}{\partial x}\left(\frac{\partial u_z}{\partial x}+\frac{\partial u_x}{\partial z}\right)+\frac{1}{\rho}\frac{\partial \eta}{\partial y}\left(\frac{\partial u_z}{\partial y}+\frac{\partial u_y}{\partial z}\right)$$

In addition, the uncompressed condition of the following equation was taken into consideration:

$$\frac{\partial^2 u_z}{\partial x^2}+\frac{\partial^2 u_z}{\partial y^2}+\frac{\partial^2 u_z}{\partial z^2}=0 \tag{14}$$

As can be seen from equations (11) – (13), they are the products of differential coefficients, and the extent of this influence was examined.

In this study, Particleworks Ver. 6 (Prometech Software, Inc. Japan), that introduced MPS, was used.

3 SIMULATION AND DISCUTTION

3.1 Slump test

The influence of the equivalent viscosity coefficient was determined by simulation of the slump test. Figure 1 shows the outline of the slump test. A cone with an inner diameter of 100 to 200 mm, an outer diameter of 166.34 to 266.34 mm, and a height of 300 mm was installed. Soil particles were placed inside the cone and gravity was applied. Subsequently, the cone was raised for 2 seconds. Table 1 shows the simulation cases and the material parameters. In this simulation, the limit of shear velocity was adopted in order to stabilize the analysis. In addition, cases in which the products of the differential coefficients were taken into consideration (termed 'Case A') and not taken into consideration (termed "Case B") were evaluated; as in equations (11) to (13). Table 2 shows the numerical results of the particle spread at 10.0 seconds. Figure 2 shows the state of the average velocity at a steady state(10 seconds). In Case 2, the height is larger and the width smaller than in Case 1. This is because the shear resistance angle is larger than in Case 1. This specimen has the influence of self-sustaining. It is thought that the general behavior of soil can be expressed even as granular matter. A comparison of Case A to Case B indicated less difference between them in this simulation. The analysis of the products of the differential coefficients solved the Navier-Stokes equation implicitly. However, this term was an explicit analysis method in our simulation that became difficult to converge. Moreover, the procedure is time consuming. It was unnecessary to consider the differential coefficient in this

model test.

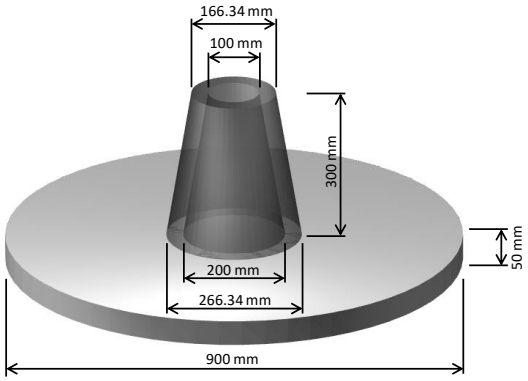

Figure 1: Layout of slump test

Table 1: Simulation cases and material parameters

	Initial viscosity coefficient η_0	Maximum viscosity coefficient η_{max}	Cohesion c (kPa)	Shear resistance angle ϕ (degrees)	Minimum shear velocity V_{min} (m/s)
Case 1	1.0	10^{100}	100	30	10^{-3}
Case 2	1.0	10^{100}	100	45	10^{-3}

Table 2: Numerical results

		Height (mm)	Width (mm)
Case 1	Case A	62.6	412.3
	Case B	75.8	384.5
Case 2	Case A	64.3	417.7
	Case B	76.5	383.7

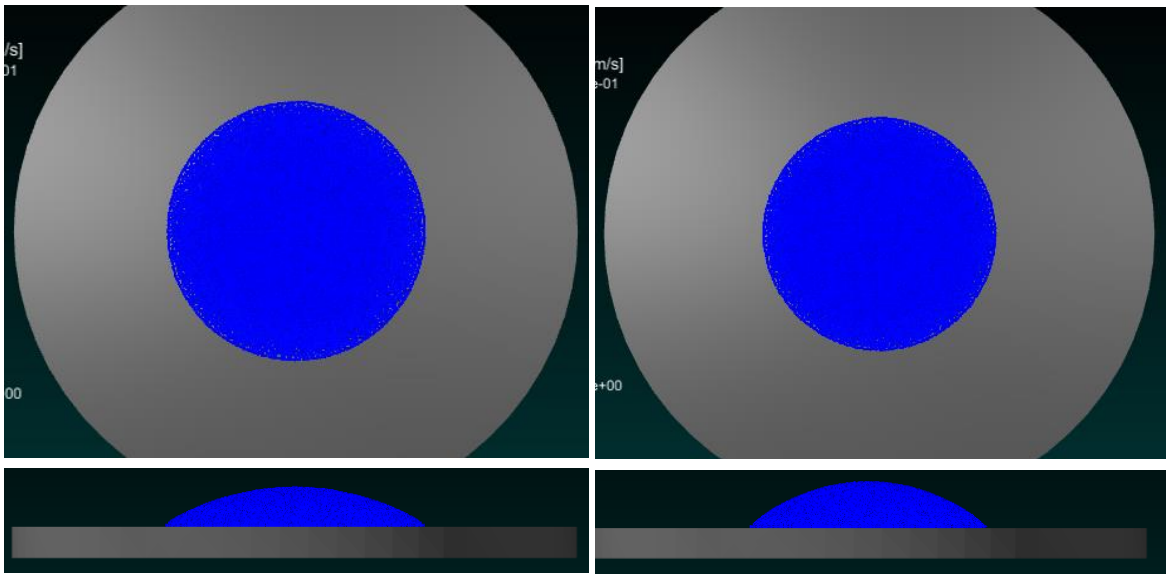

Case 1 Case 2

Case A

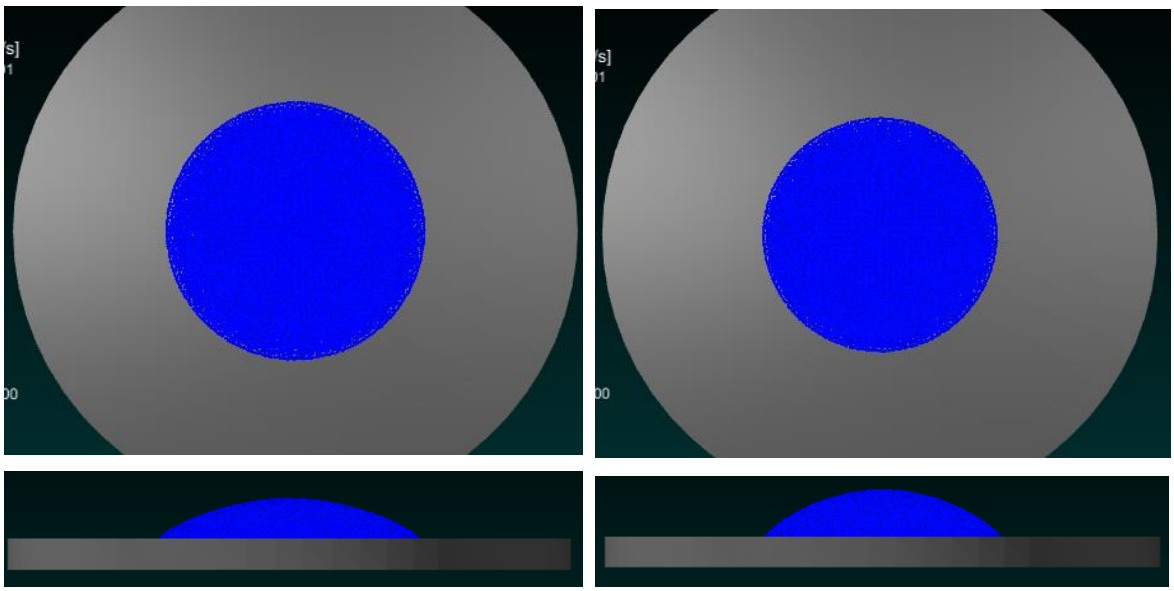

Case 1 Case 2

Case A

Figure 2: Results of the slump test

3.2 Slope flow analysis

The slope flow analysis was performed at a large scale. Figure 3 shows the outline of the slope flow analysis. It was set to the soil height of 50 m and a width of 40 m. The angle of slope is 60 degrees. In the beginning, the wall on the slope surface was set, and then that wall would be removed to begin the flow. The material parameters are the same as in Table 1. Figure 3 shows the shear strain distributions. In the case of a shear resistance angle of 30 degrees (Case 1), at 11 seconds both Case A and Case B are shown. In the case of a shear resistance angle of 40 degrees (Case 2) at 18 seconds Case A is shown, and at 40 seconds Case B is shown. In Case 1, there is less difference between Case A and Case B. The soil particles flow overall, and the especially high shear strain occurred at the surface. In Case 2 and Case A, the soil particle velocity is low, and the slope shape is retained. The shear strain occurs at the surface and then the surface flow can be seen because of a high shear resistance angle. On the other hand, in Case 2 and Case B, at the 40 second mark, the slope shape is retained and surface flow cannot be seen. When the shear resistance angle or coherence is small, the slope becomes more fluid. Once it flows, the shear rate in equation (1) increases and the effects of c and φ become relatively small. As a result, the influence of the spatial gradient of η is reduced. Contrastingly, when the shear resistance angle or coherence is large and the fluid flows slowly, the shear rate of the surface grows larger and the influence of the spatial gradient of η appears. Moreover, it appears that the effect was not as visible in the small model, as shown in Figure 1.

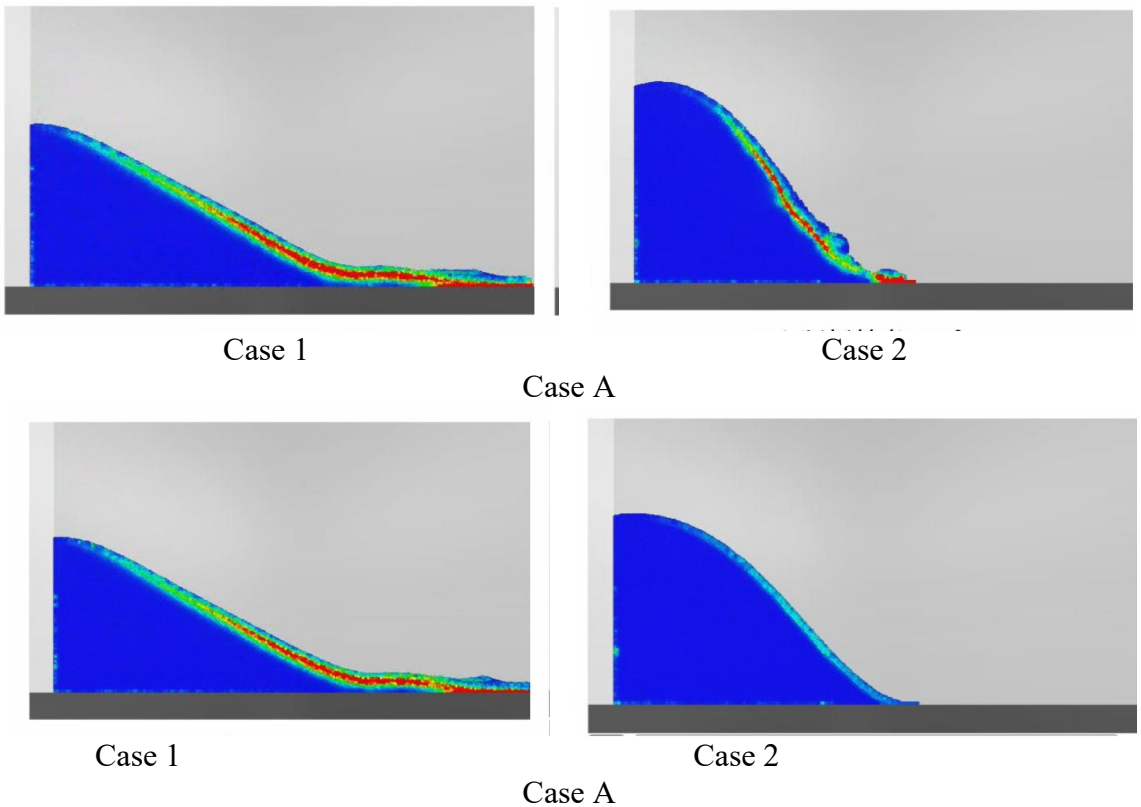

Figure 3: Results of slope flow analysis

4 REMARKS

The moving particle method was employed for the slump test and soil flow analysis. The conclusions are as follows:

- In the slump test as the shear resistance angle increases, the height increases and the width remains wide at a steady state.
- When the slope flow model with a large area is analyzed, the difference in shear resistance angle shows the difference in slope flow. It was also found that the effect of the spatial gradient of η becomes larger as the shear strain at the ground surface becomes larger.

Although aspects of the method need improvement, such as the friction of the bottom surface, the study was able to express the soil flow according to the adhesive strength of the soil and the shear resistance angle.

REFERENCES

[1] Dent JD, Lang TE 1983. A biviscous modified Bingham model of snow avalanche motion. *Ann Glaciol* 4:42–46.
[2] Soussa J, Voight B 1991. Continuum simulation of flow failures. *Geotechnique* 41:515–538.
[3] Nonoyama H, Moriguchi S, Sawada K, Yashima A 2015. Slope stability analysis using (SPH) method. *Soils Found* 55(2):458–470.
[4] Huang Y, Cheng H, Dai Z, Xu Q, Liu F, Sawada K, Moriguchi S, Yashima A 2015. SPH-based numerical simulation of catastrophic debris flows after the 2008 Wenchuan earthquake. *Bull Eng Geol Environ* 74(4):1137–1151.
[5] Koshizuka S, Oka Y 1996. Moving-particle semi-implicit method for fragmentation of incompressible fluid, *Nucl Sci Eng* 123:421–434.
[6] Moriguchi S, Borja R I, Yashima A, Sawada K 2009. Estimating the impact force generated by granular flow on a rigid obstruction. *Acta Geotechica* 4:57–71.